Proximal Side Control

DOI: 10.1002/ange.201205912

Experimental Documentation of the Structural Consequences of Hydrogen-Bonding Interactions to the Proximal Cysteine of a Cytochrome P450**

Piotr J. Mak, Yuting Yang, Sangchoul Im, Lucy A. Waskell, and James R. Kincaid**

Members of the widely distributed cytochrome P450 class of monoxygenases, or CYPs, generate highly reactive oxygen-derived intermediates that effect a diverse set of reactions, including hydroxylation and epoxidation of relatively inert substrates,[1–3] thereby facilitating such important physiological functions such as steroid biosynthesis and metabolism of pharmaceuticals.[4,5] The active-site heme b is bound by a proximal cysteine thiolate, while on the distal side the heme is presented with an intricately arranged set of residues facilitating proton transfer to ferric peroxo and ferric hydroperoxo species.[6] Substrate binding to the six-coordinate, low-spin (6cLS) ferric resting state converts it to a five-coordinate, high-spin state (5cHS) that is reduced by natural redox partners, with the resulting ferrous form then binding dioxygen. Normally, the enzymatic cycle continues on to completion (oxidation of substrate) by accepting one more electron from a reductase to generate a peroxo intermediate. Sequential delivery of two protons generates an initial hydroperoxo intermediate and then the so-called Compound I, a potent oxidizing species generally formulated as a ferryl heme π-cation radical.[1–3,7] Understandably, there is considerable interest in gaining insight into the structural factors that control the reactivity of the intermediates encountered within this cycle.[8–10] One obvious point of interest is that the strongly electron-donating axial thiolate of all CYPs and structurally related enzymes, such as nitric oxide synthases (NOSs), can promote O–O bond cleavage or impact the behavior of subsequent intermediates.[11–15] The effective negative charge on this proximal cysteine-thiolate could be fine-tuned by the nature and number of suitably positioned H-bond donors known to be present in the proximal pocket.[14–23] A direct measure of the immediate consequences of such H-bonding is documentation of the strength of the Fe–S linkage, a task most readily accomplished by resonance Raman (rR) spectroscopy, using excitation within the S→Fe charge transfer transition envelope that occurs near 360 nm in the ferric HS form.[14,16–18,24–26] Here, this direct spectroscopic method is used to interrogate active-site structural changes that accompany a single-site mutation of a truncated form of CYP2B4; i.e., the F429H variant, where the highly conserved proximal-side phenylalanine is replaced with the potentially H-bonding histidyl residue. The essential results obtained provide new definitive experimental evidence for the influence of proximal-side H-bonding on the key Fe–S linkage and its effects on the cytochrome P450 cycle.

This F429H mutant is of great interest, because the presence of this additional H-bond drastically diminished the enzyme's ability to promote O–O bond cleavage.[9] Additionally, computational studies have suggested that the mutant's heme oxygenase activity could arise as a result of a predicted weakening of the Fe–S bond strength.[15] Figure 1 shows the Soret band-excited rR spectra obtained for the substrate-free (SF) and butylated hydroxytoluene (BHT)-bound "wild-type" ferric CYP2B4 and its F429H mutant. In the case of the WT enzyme (traces A and B), substrate binding causes an almost complete conversion from a 6cLS to 5cHS state; that is, the ν_3 "spin-state marker" shifts from 1502 to 1487 cm^{-1}.[27–29] Similar behavior is documented for the F429H mutant, though the conversion is not as complete. This residual 6cLS fraction seen for the mutant might arise from decreased affinity for the substrate or from a conformational heterogeneity that increases the stability of the aquo-bound form. However, the absence of the SF form for the CO adduct (see below) argues against the former case, unless one invokes a significantly different substrate affinity between the ferric and ferrous forms. In the low-frequency region the bending modes associated with the propionate and vinyl substituents are observed near 370 cm^{-1} and 400–440 cm^{-1}, respectively. In contrast to behavior seen for bacterial P450s,[16,30] only small shifts are typically seen for microsomal mammalian CYPs such as those of interest here,[26,31] whose distal pockets are larger and more flexible.[1,2] It is noted, on the other hand, that BHT binding to both enzymes studied here does activate out-of-plane (oop) modes at 318 and 500 cm^{-1}.

The key ν(Fe–S) mode is enhanced only by excitation within the Fe–S charge transfer transition that occurs near 360 nm for the (substrate-bound) ferric HS state.[24] Thus, in Figure 2 this mode is observed as a relatively strong feature appearing at 353 cm^{-1} in the BHT-bound WT enzyme and at

[*] Dr. P. J. Mak, Prof. J. R. Kincaid
Department of Chemistry, Marquette University
Milwaukee, WI 53233 (USA)
E-mail: james.kincaid@marquette.edu
Dr. Y. Yang, Dr. S.-C. Im, Prof. L. A. Waskell
Department of Anesthesiology
University of Michigan and VA Medical Center
Ann Arbor, MI 48105 (USA)
E-mail: waskell@med.umich.edu

[**] This work was supported by the National Institutes of Health grant R01GM096117 (to J.R.K.) from the National Institutes of General Medical Sciences and by the National Institutes of Health grants R01GM035533 and R01GM094209 and a VA Merit Review Grant (to L.A.W.).

Supporting information for this article is available on the WWW under http://dx.doi.org/10.1002/anie.201205912.

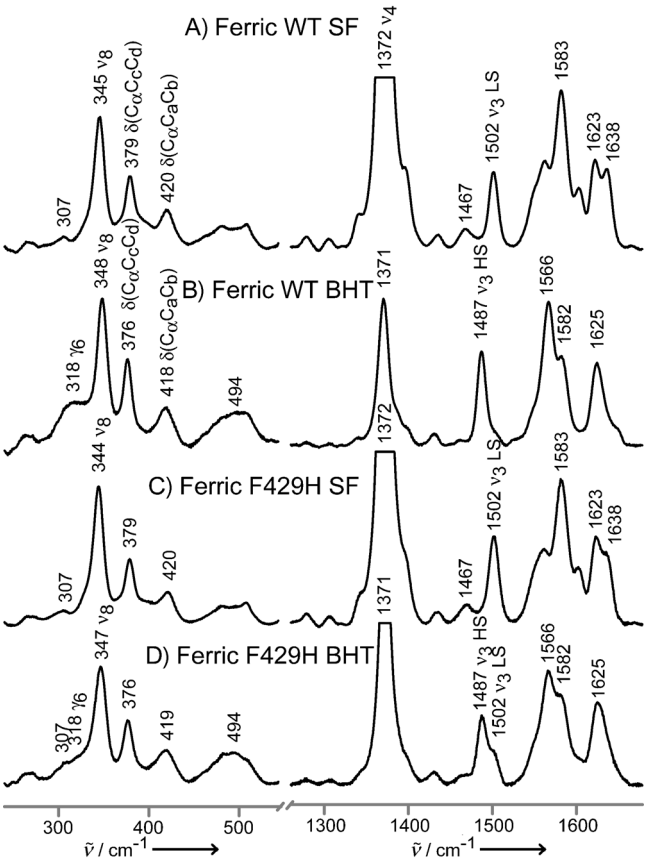

Figure 1. Low- (left) and high-frequency (right) rR spectra of ferric CYP2B4: A) wild-type substrate-free; B) wild-type BHT-bound; C) F429H mutant substrate-free; D) F429H mutant BHT-bound. Spectra measured with 406 nm excitation line and normalized to the ν_3 mode.

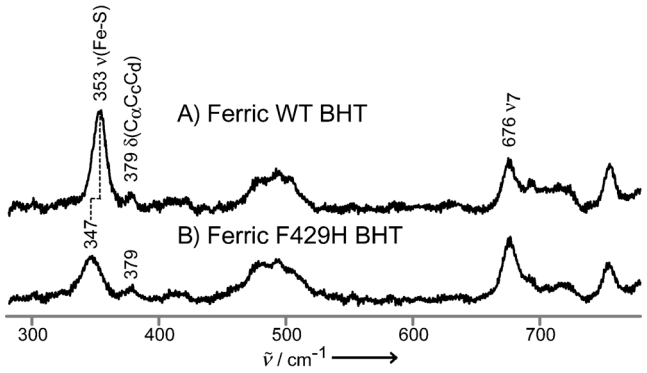

Figure 2. Low-frequency rR spectra of ferric CYP2B4: A) wild-type BHT-bound; B) F429H mutant BHT-bound. Spectra measured with 356 nm excitation line and normalized to the ν_7 mode at 676 cm^{-1}.

347 cm^{-1} for the BHT-bound CYP2B4 F429H. While the 347 cm^{-1} feature observed in the spectrum of the F429H mutant is accidently degenerate with the 347 cm^{-1} feature seen in Soret excitation (Figure 1, trace D left), the two features correspond to two different modes; i.e., the ν(Fe–S) and the ν_8 modes, respectively. Convincing evidence for this is presented in the Supporting Information, where it is shown that the observed bandwidths are substantially broader for these 353/347 cm^{-1} features than those observed for the heme modes (Figure S2).

The observed 6 cm^{-1} shift of ν(Fe–S) to lower frequency for F429H is qualitatively consistent with expectations based on the reduction of effective negative charge on the thiolate, in agreement with recent computations.[14,15] Similar earlier rR work with CYP101[17] and CYP102[16] led to unexpected results; i.e., removal of existing H-bond donors led either to no effect on the observed ν(Fe–S) frequency or an unexpected decrease,[17] while an attempt to introduce a new H-bond donor residue to the proximal pocket of CYP102 (i.e., F393H) failed to induce any observable shift of its ν(Fe–S) mode.[16] The former result was later suggested to be attributable to vibrational mode reorganization.[14] The absence of any changes on the ν(Fe–S) mode for the F393H mutant of CYP102 was interpreted as evidence that the histidyl residue was not in a proper orientation to H-bond to the proximal cysteine thiolate fragment.[16,32] Given these complications encountered in these previous rR studies, it is satisfying that the present results agree with the predicted influence on the Fe–S bond strength.[14,15]

The new H-bonding modulation of the Fe–S bond strength is also reflected in the altered electronic structure of the *trans*-axial Fe-C-O linkage of the ferrous CO adduct. Thus, as shown in Figure 3 (top), the ν(Fe–C) shifts up by 3 cm^{-1} for the mutant (i.e., 463→466 and 473→476 cm^{-1} for the SF and BHT-bound comparisons), with the ν(C–O) modes also shifting up by 5–7 cm^{-1} for the same comparisons (i.e., 1957→1962 and 1945→1952 cm^{-1}). These directly correlated shifts of the ν(Fe–C) and ν(C–O) modes, both to higher frequency, are indicative of a diminished σ-donation of the *trans*-axial proximal thiolate ligand resulting from the newly introduced H-bonding histidine residue, such behavior being in agreement with predictions made from several high-level computational studies.[14,15,33] It is noted that earlier computational work, supported with modest experimental data for models, has previously been used to argue this point for the isoelectronic ferric NO adducts.[34]

Furthermore, the behavior seen here for the vibrational modes of the Fe-C-O fragment is satisfyingly consistent with data reported for CO adducts of NOS.[23] Thus, the plots shown at the bottom of Figure 3 present data acquired for CO adducts of mammalian NOS (stars), the CO adducts of WT CYP2B4 under various conditions (open squares) and the two points obtained here for the F429H mutant of CYP2B4 (solid squares); additional data reported for bacterial NOS proteins, as well as the isoelectronic $Fe^{III}NO$ adducts of cytochromes P450 and model compounds, are given in Figure S3 of Supporting Information. The inverse correlations of the ν(Fe–C) and ν(C–O) modes are generally accepted to reliably reflect variations in polarity of the distal heme pocket,[33,35] with displacements from one another along the vertical direction being the result of differences in the strength of the proximal ligand. Thus, the displacement of the NOS line from the CYP2B4 line arises because the Fe–S bonds of the NOSs are weakened by the presence of an H-bond from a conserved tryptophan residue in the proximal

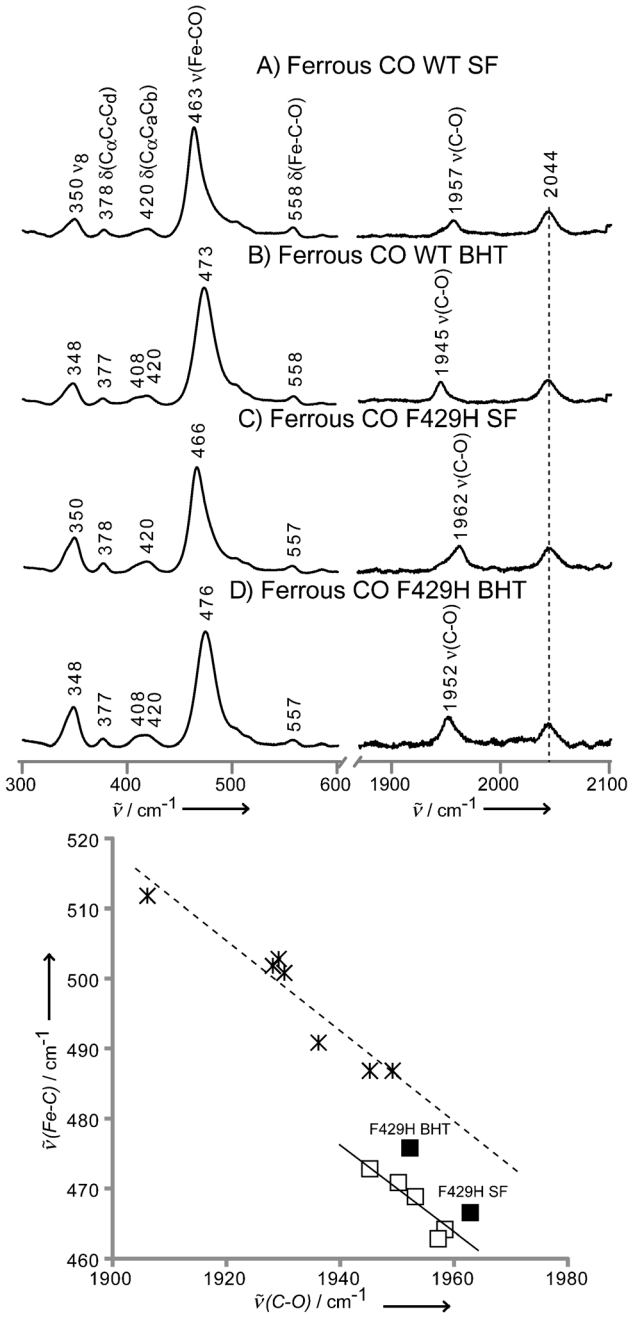

Figure 3. Low- (left) and high-frequency (right) rR spectra of ferrous CO adducts of CYP2B4: A) wild-type substrate-free; B) wild-type BHT-bound; C) F429H mutant substrate-free; D) F429H mutant BHT-bound. Spectra measured with 442 nm excitation line and normalized to the ν_7 and ν_4 modes for low- and high-frequency region, respectively. The bottom graph shows linear correlation between ν(Fe–C) and ν(C–O) frequencies, the open squares represent wild-type truncated CYP2B4,[40] the solid squares indicate points for F429H mutants, and the stars show mammalian NOSs.[37–39]

pocket; i.e., their ν(Fe–S) stretching frequencies generally occur near 338 cm^{-1},[36] approximately 12–14 cm^{-1} lower than for cytochromes P450. As can be seen in Figure 3, the points derived for the F429H mutant of CYP2B4 indeed are shifted towards the line for the NOS proteins, a shift entirely consistent with the observed 6 cm^{-1} lowering of the ν(Fe-S) for this mutant.[37–39]

Finally, it is noteworthy that the remarkable structural sensitivity of the rR technique reveals small, but clearly detectable, mutation-induced changes for particular heme modes of the F429H mutant. A complex difference pattern (Figure 4, trace C) is obtained when comparing the rR spectra for the SF forms of ferrous CO adducts of the WT and F429H

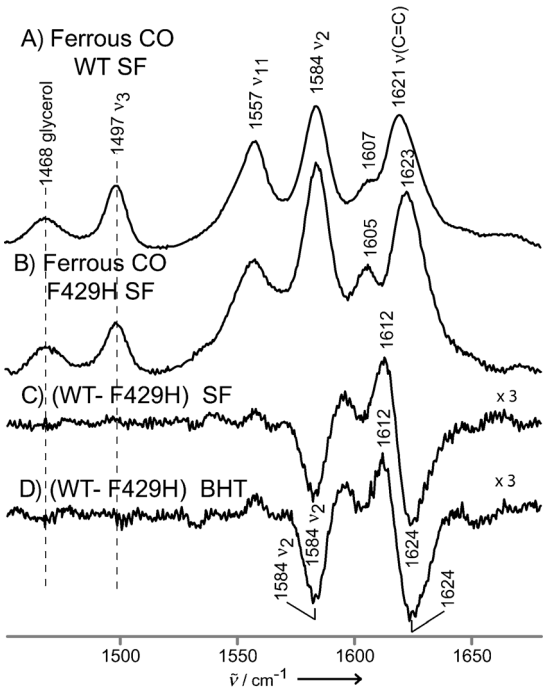

Figure 4. High-frequency rR spectra of ferrous CO adducts of substrate-free CYP2B4: A) wild-type; B) F429H mutant. Spectra were normalized to the glycerol mode at 1468 cm^{-1}. The traces (C) and (D) are difference traces of ferrous CO adducts of CYP2B4 wild-type and 429H mutant in substrate-free form (C) and in BHT-bound state (D).

mutant. A similar difference plot obtained for the pair of BHT-bound forms is given in trace D. These data show that, while the mutation does not significantly change the basic heme structure, as reflected in the constancy of the core-sensitive ν_3 and ν_{11} modes, changes are evident in the spectral region associated with the ν(C=C) modes of the peripheral vinyl groups. The most reasonable interpretation of these difference patterns is that the vinyl mode envelope is shifted to slightly higher frequency, behavior which is consistent with out-of-plane displacement of the vinyl groups.[16] This displacement diminishes the conjugation of the vinyl groups with the heme macrocyle π-system, with the result that the ν_2 core mode, associated with stretching of the C_β–C_β bonds of the pyrrole ring to which the vinyls are attached,[28] is also altered, experiencing an increased resonance enhancement. Significantly, all of these changes are observed for modes of molecular fragments localized at or near the 2- and/or 4-vinyl groups and are therefore entirely consistent with the proposed interaction of the newly introduced histidyl imida-

zole with the pyrrole A-ring, based on inspection of the recently acquired X-ray crystal structure of the mutant.[45]

In summary, the present results show that the newly introduced H-bond does indeed lead to a shift of the ν(Fe-S) stretching mode to lower frequency, documenting a weakening of this bond, as predicted by theory.[14,15] Furthermore, the impact of this modulation of Fe–S bond strength is transmitted to the heme iron linkage with a *trans*-axial diatomic ligand (CO), as reflected in the observed behavior of the ν(Fe–C) and ν(C–O) modes of the Fe-C-O fragment,[23,41] such electronic effects holding potential implications for functional properties. Finally, changes in certain heme vibrational modes provide convincing evidence for the presence of an intimate interaction between the replacement residue, 429H, and the heme pyrrole A-ring, a structural feature that is suggested from inspection of preliminary X-ray crystallographic data.[45]

Experimental Section

Plasmid for the truncated mutant was constructed from pLW01 wild-type full-length P4502B4 plasmid.[42] The cDNA coding for the 19 amino acids at the N-terminus (amino acids 3–21 of WT CYP2B4) were removed using NcoI restriction sites which had been inserted at position 3 and 21 by site-directed mutagenesis. After removing the cDNA between the two NcoI sites, the remainder of the plasmid was religated by T4 DNA ligase (Invitrogen, NY). The following mutations, E2A, G22K, H23K, P24T, K25S, A26S, H27K, R29K, H226Y and F429H were then introduced into the Δ3–21 WT CYP2B4, using a QuikChange Site-Directed Mutagenesis Kit (Stratagene) to generate the F429H mutant of the truncated form of CYP2B4. The truncated form of CYP2B4 (all of the mutations indicated above, minus the F429H mutation), considered WT above, is the form which had been previously engineered to allow successful crystallization when bound to different compounds.[43]

The plasmid pLW01 CYP450 2B4 F429H with cDNA for the mutant or WT CYP2B4 was transformed into C41 (DE3) cells. The cells were grown in TB medium at 23 °C and induced with IPTG, supplemented with δ-aminolevulinic acid at induction and ethanol 30 min after induction. The induced cell culture was harvested ca. 120 h after induction.

The protein samples were isolated and purified as previously described.[44] Butylated hydroxytoluene (BHT) was added to all buffers to prevent conversion to cytochrome P420 during purification. The protein was eluted from hydroxyapatite column using buffer containing 0.4 M K_2HPO_4/KH_2PO_4 pH 7.4 and 20% glycerol. The purified protein was diluted into a final buffer containing 20% glycerol and 0.1 M K_2HPO_4/KH_2PO_4 pH 7.4 and concentrated to ca. 1 mM using 50000 MWCO VivaSpin 20.

The rR measurements: All samples are ca. 0.4 mM in heme. All further details, including solution conditions and spectrometer parameters are given in the Supporting Information.

Received: July 24, 2012
Published online: September 11, 2012

Keywords: biophysics · heme proteins · oxidoreductases · Raman spectroscopy

[1] *Cytochrome P450: Structure, Mechanism and Biochemistry*, 3rd ed. (Ed.: P. R. Ortiz de Montellano), Kluwer/Plenum, New York, **2004**.
[2] *Metal Ions in Life Sciences*, *Vol. 3* (Eds.: A. Sigel, H. Sigel, R. K. O. Sigel), Wiley, Chichester, **2007**.
[3] M. J. Coon, *Annu. Rev. Pharmacol. Toxicol.* **2005**, *45*, 1 – 25.
[4] F. P. Guengerich, *Chem. Res. Toxicol.* **2008**, *21*, 70 – 83.
[5] P. F. Hollenberg, U. M. Kent, N. N. Bumpus, *Chem. Res. Toxicol.* **2008**, *21*, 189 – 205.
[6] I. G. Denisov, T. M. Makris, S. G. Sligar, I. Schlichting, *Chem. Rev.* **2005**, *105*, 2253 – 2277.
[7] J. Terner, V. Palaniappan, A. Gold, R. Weiss, M. M. Fitzgerald, A. M. Sullivan, C. M. Hosten, *J. Inorg. Biochem.* **2006**, *100*, 480 – 501.
[8] R. Davydov, I. D. G. Macdonald, T. M. Makris, S. G. Sligar, B. M. Hoffman, *J. Am. Chem. Soc.* **1999**, *121*, 10654 – 10655.
[9] R. Davydov, R. Razeghifard, S.-C. Im, L. Waskell, B. M. Hoffman, *Biochemistry* **2008**, *47*, 9661 – 9666.
[10] I. G. Denisov, P. J. Mak, T. M. Makris, S. G. Sligar, J. R. Kincaid, *J. Phys. Chem. A* **2008**, *112*, 13172 – 13179.
[11] J. Rittle, M. T. Green, *Science* **2010**, *330*, 933 – 937.
[12] S. Shaik, S. Cohen, Y. Wang, H. Chen, D. Kumar, W. Thiel, *Chem. Rev.* **2010**, *110*, 949 – 1017.
[13] K. L. Stone, R. K. Behan, M. T. Green, *Proc. Natl. Acad. Sci. USA* **2006**, *103*, 12307 – 12310.
[14] M. G. I. Galinato, T. Spolitak, D. P. Ballou, N. Lehnert, *Biochemistry* **2011**, *50*, 1053 – 1069.
[15] D. Usharani, C. Zazza, W. Lai, M. Chourasia, L. Waskell, S. Shaik, *J. Am. Chem. Soc.* **2012**, *134*, 4053 – 4056.
[16] Z. Chen, T. W. B. Ost, J. P. M. Schelvis, *Biochemistry* **2004**, *43*, 1798 – 1808.
[17] S. Yoshioka, T. Tosha, S. Takahashi, K. Ishimori, H. Hori, I. Morishima, *J. Am. Chem. Soc.* **2002**, *124*, 14571 – 14579.
[18] J. Lang, J. Santolini, M. Couture, *Biochemistry* **2011**, *50*, 10069 – 10081.
[19] F. Ogliaro, S. Cohen, S. P. de Visser, S. Shaik, *J. Am. Chem. Soc.* **2000**, *122*, 12892 – 12893.
[20] F. Ogliaro, S. P. de Visser, S. Shaik, *J. Inorg. Biochem.* **2002**, *91*, 554 – 567.
[21] T. L. Poulos, B. C. Finzel, A. J. Howard, *J. Mol. Biol.* **1987**, *195*, 687 – 700.
[22] K. G. Ravichandran, S. S. Boddupalli, C. A. Hasemann, J. Peterson, J. Deisenhofer, *Science* **1993**, *261*, 731 – 736.
[23] C. A. Hasemann, K. G. Ravichandran, S. S. Boddupalli, J. Peterson, J. Deisenhofer, *Structure* **1995**, *3*, 41 – 62.
[24] P. M. Champion, B. R. Stallard, G. C. Wagner, I. C. Gunsalus, *J. Am. Chem. Soc.* **1982**, *104*, 5469 – 5472.
[25] J. Sabat, D. J. Stuehr, S.-R. Yeh, D. L. Rousseau, *J. Am. Chem. Soc.* **2009**, *131*, 12186 – 12192.
[26] P. J. Mak, S.-C. Im, H. Zhang, L. A. Waskell, J. R. Kincaid, *Biochemistry* **2008**, *47*, 3950 – 3963.
[27] T. Kitagawa, Y. Mizutani, *Coord. Chem. Rev.* **1994**, *135/136*, 685 – 735.
[28] *Biological Applications of Raman Spectroscopy*, *Vol. III* (Ed.: T. G. Spiro), Wiley, New York, **1988**.
[29] J. R. Kincaid in *Porphyrin Handbook*, *Vol. 7* (Eds.: K. M. Kadish, K. M. Smith, R. Guilard), Academic Press, San Diego, **2000**, pp. 225 – 291.
[30] P. J. Mak, D. Kaluka, E. M. Manyumwa, H. Zhang, T. Deng, J. R. Kincaid, *Biopolymers* **2008**, *89*, 1045 – 1053.
[31] P. J. Mak, I. G. Denisov, Y. V. Grinkova, S. G. Sligar, J. R. Kincaid, *J. Am. Chem. Soc.* **2011**, *133*, 1357 – 1366.
[32] T. W. B. Ost, A. W. Munro, C. G. Mowat, P. R. Taylor, A. Pesseguiero, A. J. Fulco, A. K. Cho, M. A. Cheesman, M. D. Walkinshaw, S. K. Chapman, *Biochemistry* **2001**, *40*, 13430 – 13438.
[33] C. Xu, M. Ibrahim, T. G. Spiro, *Biochemistry* **2008**, *47*, 2379 – 2387.
[34] F. Paulat, N. Lehnert, *Inorg. Chem.* **2007**, *46*, 1547 – 1549.
[35] X.-Y. Li, T. G. Spiro, *J. Am. Chem. Soc.* **1988**, *110*, 6024 – 6033.

[36] J. P. M. Schelvis, V. Berka, G. T. Babcock, A. Tsai, *Biochemistry* **2002**, *41*, 5695 – 5701.
[37] J. Wang, D. J. Stuehr, M. Ikeda-Saito, D. L. Rousseau, *J. Biol. Chem.* **1993**, *268*, 22255 – 22258.
[38] B. Fan, J. Wang, D. J. Stuehr, D. L. Rousseau, *Biochemistry* **1997**, *36*, 12660 – 12665.
[39] J. Wang, D. J. Stuehr, D. L. Rousseau, *Biochemistry* **1997**, *36*, 4595 – 4606.
[40] P. J. Mak, H. Zhang, P. F. Hollenberg, J. R. Kincaid, *J. Am. Chem. Soc.* **2010**, *132*, 1494 – 1495.
[41] T. G. Spiro, I. H. Wasbotten, *J. Inorg. Biochem.* **2005**, *99*, 34 – 44.
[42] A. Bridges, L. Gruenke, Y. T. Chang, I. A. Vakser, G. Lowe, L. Waskell, *J. Biol. Chem.* **1998**, *273*, 17036 – 17049.
[43] E. E. Scott, M. A. White, Y. A. He, E. F. Johnson, C. D. Stout, J. R. Halpert, *J. Biol. Chem.* **2004**, *279*, 27294 – 27301.
[44] A. S. Saribas, L. Gruenke, L. Waskell, *Protein Expression Purif.* **2001**, *21*, 303 – 309.
[45] L. Waskell, unpublished results.

